Unraveling the Rheology of Nanocellulose Aqueous Suspensions: A Comprehensive Study on Biomass-Derived Nanofibrillated Cellulose

Mingyue Miao,[†] Fei Wang,[†] Longchen Tao, Chenchen Dai, Yu Liu, Shujuan Han, Qing Li[*], Wenshuai Chen[*], Ping Lu[*]

[*] Q. Li, F. Wang, L. Tao, S. Han, C. Dai, J. Huang, Prof. W. Chen, Prof. H. Yu
Key laboratory of Bio-based Material Science and Technology, Ministry of Education, Northeast Forestry University
Harbin 150040, P. R. China
E-mail: liqing007007@126.com; chenwenshuai@nefu.edu.cn

P. Lu, Department of Chemistry and Biochemistry, Rowan University, Glassboro, New Jersey 08028, United States
E-mail: lup@rowan.edu

[**] This work was supported in part by "the Fundamental Research Funds for the Central Universities" (Grant No. 2572021CG01 and No. 2572019BB03).

† These authors contributed equally to this work.

ABSTRACT

The rheological properties of nanocellulose aqueous suspensions play a critical role in the development of nanocellulose-based bulk materials. High-crystalline, high-aspect ratio, and slender nanofibrillated cellulose (NFC) were extracted from four biomass resources. The cellulose nanofibers and nanofiber bundles formed inter-connected networks in the NFC aqueous suspensions. The storage moduli of the suspensions with different concentrations were higher than their corresponding loss moduli. As the concentration increased, the storage and loss modulus of NFC dispersion increased. When the shear rate increased to a certain value, there were differences in the changing trend of the rheological behavior of NFC aqueous suspensions derived from different biomass resources and the suspensions with different concentrations. At higher shear rates, the NFC entanglement networks in some dispersions were somewhat damaged. NFC dispersion's storage and loss modulus increased when the temperature rose to nearly 80 °C. We hope this study can deepen the understanding of the rheological properties of NFC colloids derived from different biomass resources.

KEYWORDS

Biomass resources; Nanofibrillated cellulose; High-pressure homogenizer; Suspension; Rheology properties

1 Introduction

With the increasing attention to carbon-neutral strategies, developing and utilizing sustainable low-carbon resources has become a hot topic in material science fields [1]. Cellulose nanofibrils that support the plant cell walls exhibit tremendous potential in developing sustainable structural materials owing to their unique nanofiber structure and performance advantages [2-6].To release cellulose nanofibrils from biomass resources, chemical pretreatment is needed to remove the lignin and large amounts of hemicellulose, resulting in chemically purified cellulose pulps [7]. Nanofibrillated cellulose (NFC) was individualized by nanofibrillation of the cellulose pulps using various equipment, such as a high-pressure homogenizer [8], grinder [9], high-intensity ultrasonicator [7, 10-13], high-speed blender [14], beads mill [15], and twin-screw extruder [16]. The as-isolated NFC is very long and ultrafine, with a high aspect ratio and crystallinity. Due to the differences in the structure of elementary fibrils in different biomass resources, there are differences in the structure and nanofibrillation degree of NFC prepared using different disintegration methods and from different raw materials.

The surface of NFC exposes a large number of hydroxyl groups. For some NFC extraction methods, the cellulose pulps were chemically modified before disintegration. The surface of the as-produced NFC also contains other types of hydrophilic groups, such as carboxylic groups [17]. NFC is thus well dispersed in water. The dispersion state of NFC in water depends on its structure, surface groups, nanofibrillation degree, and solid concentration. For example, for the < 0.2 wt% NFC aqueous suspension prepared by nanofibrillation of the wood cellulose pulps using a high-intensity ultrasonicator, the NFC may precipitate at the bottom of the beaker after the suspension has been standing for a period [12]. In contrast, TEMPO-oxidized NFC aqueous dispersion is very stable. Even if the suspension was placed for a long time, NFC would still be evenly dispersed in water [17]. Therefore, different types of NFC dispersed in water exhibit various colloidal states under different conditions.

The rheological properties of NFC play an essential role in the fabrication of NFC-based bulk materials. The long and hydrophilic NFC interwoven into a network structure in water and interacted via hydrogen bonds and van der Waals forces. Some processing technologies, such as printing and extrusion [18, 19], have strict requirements for the storage modulus, loss modulus, and loss angle tangent of the NFC dispersions. There is a great deal of research works on the rheological properties of NFC suspensions and the dispersions composed of NFC and other active components [20-24]. The rheological properties of NFC colloids with different solid contents have been studied at different angular frequencies and temperatures. However, due to the differences in the structure and characteristics of NFC obtained from different raw materials and using different nanofibrillation methods, the impact of different NFC building blocks on the rheological properties of their aqueous suspensions is still unclear.

Herein, we systematically studied the rheological properties of the aqueous suspensions of NFC isolated from biomass resources. To eliminate the influence of preparation methods on the structure of NFC, we used the same method of chemical pretreatment combined with nanofibrillation using a high-pressure homogenizer to extract high crystalline NFC from wood, bagasse, wheat straw, and bamboo. Then, we conducted a comparative study on the rheological properties of NFC aqueous suspensions obtained from the four biomass resources. The

rheological properties of 0.2 wt% and 0.5 wt% NFC dispersions were also compared. We found that the storage modulus of the four NFC aqueous suspensions is greater than that of the loss modulus at room temperature. Increasing the concentration increased the storage modulus and loss modulus of the dispersions. There were certain differences in the rheological properties of different types of NFC suspension when the shear rate and temperature changed.

2 Materials and Methods

2.1 Raw Materials

Powders from poplar wood, bagasse, wheat straw, and bamboo, which were sieved below 60 mesh, were used as the raw materials. All samples were washed with distilled water and subsequently oven-dried at 60 °C, and then sealed storage at room temperature. Potassium hydroxide, acetic acid, sodium chlorite, and other chemicals were purchased from Aladdin Reagent Co., Ltd, which were all laboratory grade without further purification.

2.2 NFC Extraction

The NFC extraction process is mainly divided into two steps: chemical pretreatment and mechanical processing. In the chemical pretreatment stage, sodium chlorite treatment and potassium hydroxide treatment were used to removed lignin and large amounts of hemicelluloses from the powders of the biomass resources. The remaining products were chemically purified cellulose pulps. Next, the cellulose pulp dispersions with solid concentration of 0.2 wt% and 0.5 wt% were prepared. The cellulose pulps were first nanofibrillated using an ultrasonic generator (JY99-IIDN, Ningbo Scientz Biotechnology Co., Ltd., China) at 800 W for 20 min, with protect by an ice-water bath. The as-obtained water suspensions were further nanofibrillated using a high-pressure homogenizer (APV-2000 homogenizer, SPW Corp., Charlotte, NC, USA) for 20 min, yielding NFC aqueous suspensions. The high-pressure homogenizer was set at an operating pressure of 8~10 MPa for homogenizing valve 1 and 35~40 MPa for homogenizing valve 2.

2.3 TEM Observation

The structure of NFC was characterized by a transmission electron microscope (TEM) (FEI Tecnai G2 electron microscope) at an accelerating voltage of 80 kV. One drop of NFC suspension was dropped onto the carbon-coated electron microscopy grids and naturally dried. Subsequently, 1 wt% phosphotungstic acid was dropped on the sample and naturally dried before the TEM observation. TDYV5.2 microscope image analysis system (Beijing Tianhong Precision Instrument Technology Co., Ltd., China) was used to test the width of NFC in the TEM images.

2.4 SEM Observation

The structure of the samples was characterized by scanning electron microscope (SEM) (Quanta 200, FEI, USA). The samples were pasted onto the metal stage by conductive adhesive. Then, the surface and side of the samples were sprayed by gold using an ion sputter coater. The observation conditions of the SEM were set at 12.5 and 20 kV.

2.5 Magnifying glass observation

The petri dish containing NFC water suspension was placed on a light microscope and illuminate the light from the bottom. Then, the magnifying glass above was used to observe the sample in a vertical direction, and digital photographs were taken.

2.6 Tyndall effect observation

A red laser light was irradiated from one side of the vial containing NFC aqueous dispersion, and digital photographs of the vial were taken.

2.5 Crystal Structure Analysis

The X-ray diffraction (XRD) patterns of the samples from various biomass resources were characterized by using a D/max 2200 X-ray diffractometer (RIGAKU, Japan) at 40 kV and 30 mA with nickel filtered copper Kα radiation (k = 0.154 nm). The test range was set as follows: the range of 2θ set as 10°~40° and the scanning rate was 5° min^{-1}.

According to the Segal method [25], the crystallinity of the samples was calculated as follows:

$$\mathrm{CI}(\%) = \frac{I_{200} - I_{am}}{I_{200}} \times 100\%$$

Among them, I_{200} stands for the height of the 200 peak (I_{200}, 2θ = 22.6°), which represents both crystalline and amorphous parts, and I_{am} stands for the lowest height between the 200 and 110 peaks (I_{am}, 2θ = 18°), and represents the amorphous part.

2.6 Dynamic Rheology Analysis

The dynamic rheological properties of the NFC suspensions were investigated by using a stress-controlled AR-2000 rheometer (TA Instruments, USA) with a plate/plate geometry (diameter 40 mm, gap 1 mm). In this experiment, the strain amplitude of both concentrations was set to 0.5. In the angular frequency sweeps, the test range was performed as follows: the angular frequency scanning range is 0.1~100 rad s^{-1}, and the corresponding temperature was 25 °C. In the temperature sweeps, the temperature scanning range was 20~80 °C with a heating rate of 1 °C min^{-1}, and the corresponding angular frequency was 1 Hz. Low viscosity paraffin oil was used to seal the NFC suspensions during temperature scanning.

3 Results and Discussion

3.1 Structures of Cellulose Pulps

Wood, bagasse, wheat straw and bamboo are used as raw materials for producing NFC. Lignin and large amounts of hemicellulose were removed by chemically purified treatment using sodium chlorite and potassium hydroxide, respectively, leading to the generation of purified cellulose pulps (PCPs) (Figure 1). After purification, the cells of different biomass resources are mainly split into long and irregular fibers. The fibers are mainly existed with micron-scaled size. Bamboo PCPs also have square-like tissues that derived from the parenchyma cells of bamboo. In the present situation, high-aspect ratio cellulose nanofibers are

arranged in PCPs and not be extracted. However, the removal of matrix generates lots of "pores" and loose the inner-structures of PCPs. After the subsequent treatment by nanofibrillation process using a high intensity ultrasonicator, the PCPs were disintegrated. To further improve the nanofibrillation degree, the as-generated suspensions were further individualized using a high-pressure homogenizer, and high-aspect ratio NFC was produced.

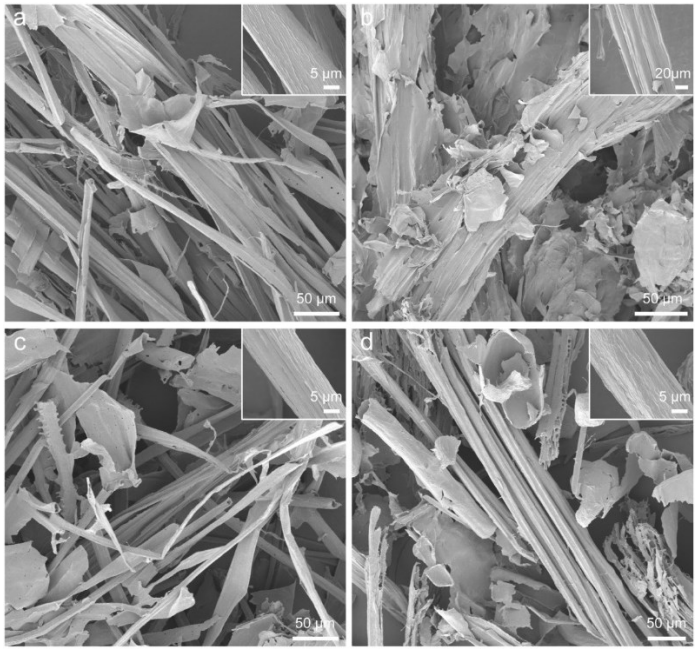

Figure 1. SEM images of the cellulose pulps of (a) wood, (b) bagasse, (c) wheat straw and (d) bamboo.

3.2 Structures of NFC

The single nanofibers of the NFC derived from different biomass resources are long and quite slender with width of 3~5 nm (Figure 2), which are recognized as the elemental fibrils of the original resources.

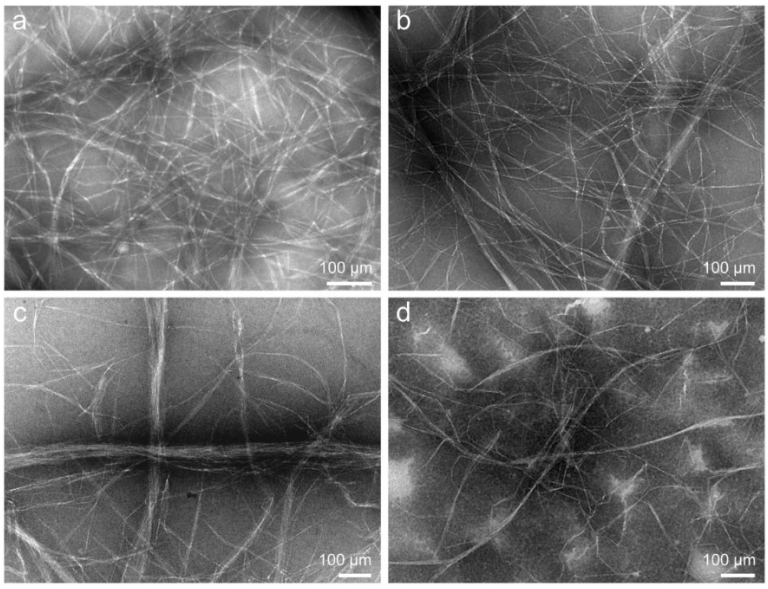

Figure 2. TEM images of NFC isolated from the PCPs of (a) wood, (b) bagasse, (c) wheat straw and (d) bamboo.

Due to the strong hydrogen bond interaction between the adjacent nanofibers within the cellulose pulps, large amounts of nanofiber bundles were existed after mechanical nanofibrillation. From the TEM observation, the structure of nanofibers and bundles separated from different biomass resources is similar. In the NFC suspension, the individualized nanofibers and bundles were uniformly dispersed in water and interconnected into web-like structures, and forms stable colloid suspensions.

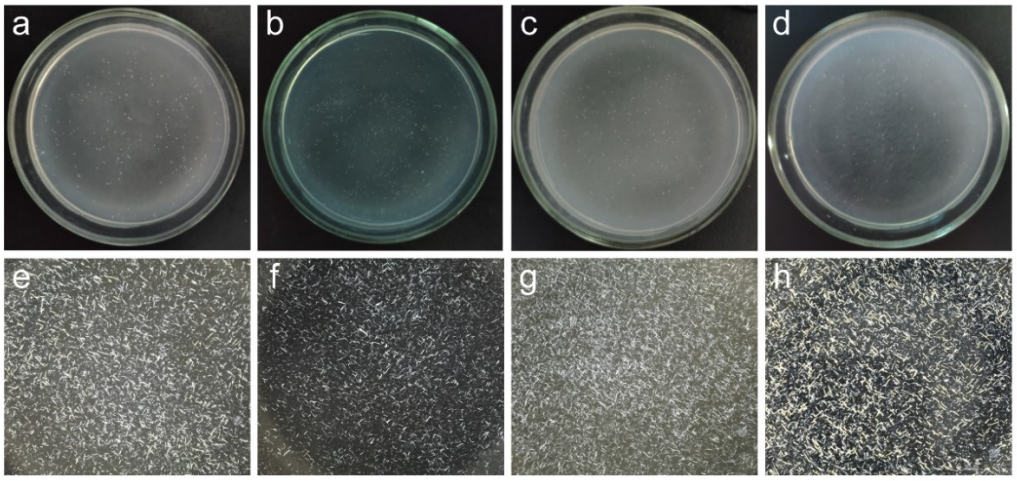

Figure 3. Digital photographs of the NFC suspensions of (a, e) wood, (b, f) bagasse, (c, g) wheat straw, and (d, h) bamboo, observing from a magnifier.

When observing the NFC aqueous suspension illuminated from the bottom using a magnifying glass, bundle-like crystal aggregates were observed and the aggregates were uniform dispersed in all the suspensions (Figure 3), indicating the formation of strong interconnected networks in the NFC suspensions. When irradiating the NFC suspensions using laser from one side of the bottle, all the suspensions scattered light and Tyndall effect was observed (Figure 4), further confirming that the 0.5 wt% NFC suspensions from various biomass resources were stable.

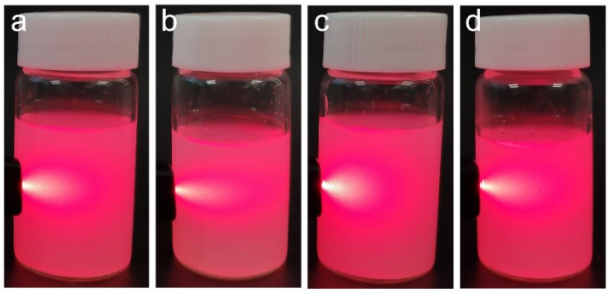

Figure 4. Digital photographs of laser irradiation from one side of a vial containing NFC water suspension of (a) wood, (b) bagasse, (c) wheat straw, and (d) bamboo.

3.3 XRD Analysis

Figure 5 shows the XRD curves of the raw materials, PCPs and NFC of wood, bagasse, wheat straw and bamboo. All the curves have peaks at 2θ around 16.5° and 22.5°, indicating all the samples have a typical cellulose I crystalline structure. Thus, the chemical purification process and the mechanical nanofibrillation process do not change the crystal type of the

cellulose. The crystallinities of the original wood, bagasse, bamboo and wheat straw are 75%, 51%, 67% and 66%, respectively. Owing to the removal of lignin and large amounts of hemicellulose, the crystallinities of PCPs of wood, bagasse, bamboo and wheat straw increased to 80%, 68%, 76% and 69%, respectively. After nanofibrillation using a high intensity ultrasonicator followed by a high-pressure homogenizer, the crystallinities of NFC of wood, bagasse, bamboo and wheat straw are 82%, 67%, 78% and 71%, respectively. Thus, it can be confirmed that the stable NFC aqueous suspension is mainly organized by high crystalline cellulose nanofibers and bundles.

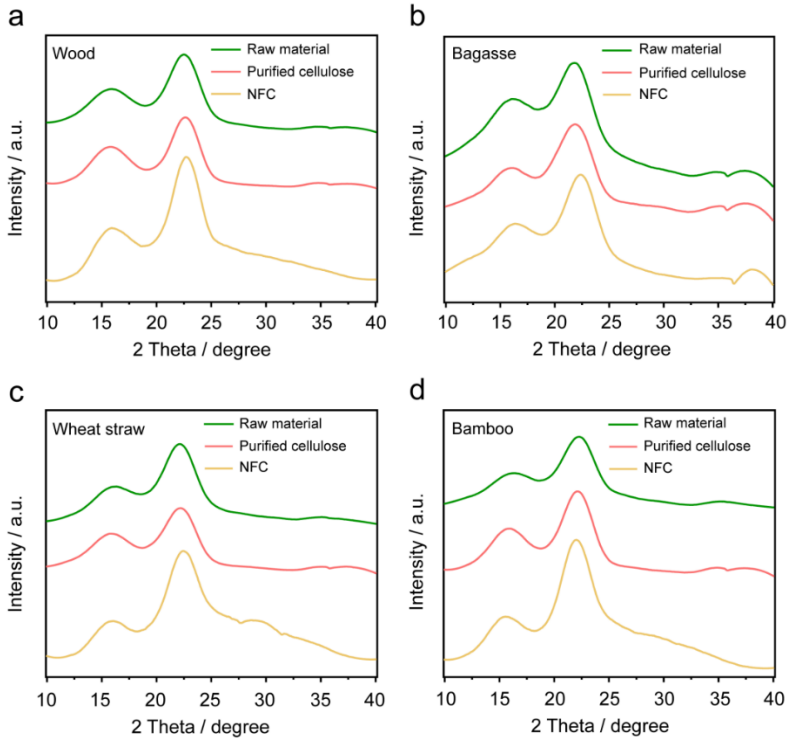

Figure 5. XRD patterns of the NFC, PCPs, and raw materials of (a) wood, (b) bagasse, (c) wheat straw, and (d) bamboo.

3.4 Comparative Study of Dynamic Rheology Properties

Suspensions with different solid contents of various biomass resources-derived NFC suspensions were characterized with increasing the angle frequency sweep and the results are shown in Figure 6. At the low frequency region, the storage modulus (*G'*) of all the samples is higher than the loss modulus (*G''*). And the *G'* and *G''* of the NFC water suspensions with a solid concentration of 0.5 wt% are higher than that of 0.2 wt%. For wood NFC suspension with a solid concentration of 0.2 wt%, the *G'* curves showed two distinct regions. At a low shearing rate, the G' is stable with increasing the angle frequency. As the angular frequency increases, the curve enters the second region. The higher the angular frequency, the greater the *G'*. At an angular frequency of 100 rad s^{-1}, the *G'* of the wood NFC aqueous suspension reaches 48 Pa. NFC aqueous suspensions derived from wheat straw and bamboo with a solid concentration of 0.2 wt% also exhibit a similar trend; this phenomenon is mainly due to the formation of a strong entanglement network between the high aspect ratio NFC when the shear rate increases to a certain value, which improves the shear resistance and thus increases the *G'*. However, the 0.2 wt% bagasse-derived NFC aqueous suspension exhibits different changing trend. As the shear

rate increases, the *G'* of the NFC suspension slowly increases. When the shear rate exceeds 10 rad s^{-1}, the storage modulus of the sample decreases rapidly, indicating that bagasse-derived NFC does not form a strong entanglement network at high shear rates. The *G''* of all the NFC aqueous suspensions increases with the increase of shear rate, but when the shear rate increases to a certain value, the numerical stability of the *G''* becomes poor. Several discrete points are found in Figure 6a, c, e, g.

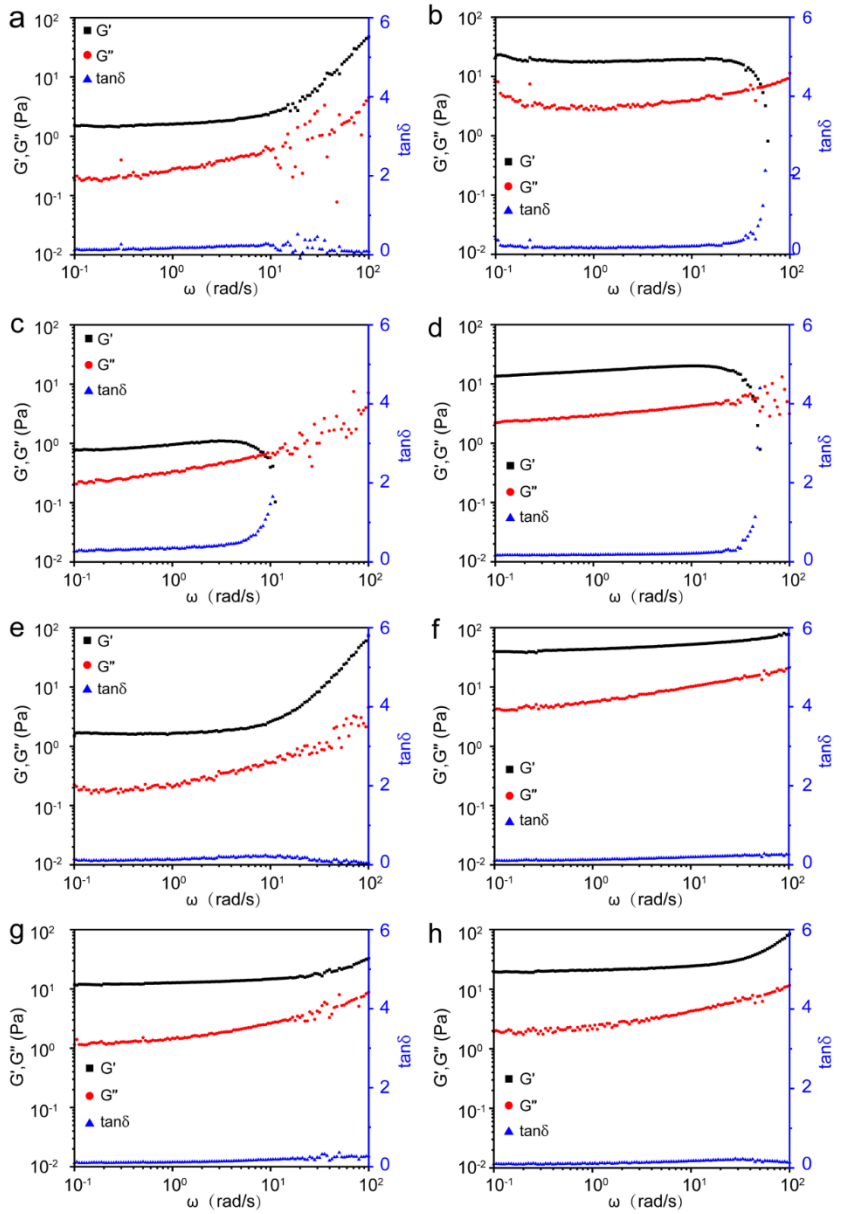

Figure 6. Rheological properties of 0.2 wt% (a, c, e, g) and 0.5 wt% (b, d, f, h) NFC suspensions with increasing the angular frequency. (a, b) wood, (c, d) bagasse, (e, f) wheat straw, and (g, h) bamboo.

When the concentration of the NFC aqueous suspension is increased to 0.5 wt%, the dispersions contains more NFC at the same volume. The NFC forming a more stable inter-connected network. The *G'* and *G''* of all samples are higher than that of 0.2 wt% NFC suspension. The *G'* of all the 0.5 wt% NFC suspensions is higher than that of the *G''*. Both *G'* and *G''* increase as the shear rate increases. However, when the shear rate is higher than 26.6

rad s^{-1} and 28.2 rad s^{-1}, the *G'* of NFC suspensions derived from wood and bagasse begins to decrease, indicating that the entanglement network structure of nanofibers in NFC dispersions is somewhat destroyed at high shear rates. The *G'* of NFC aqueous dispersions derived from wheat straw and bamboo continues to increase. When the shear rate is 100 rad s^{-1}, the *G'* of the two dispersions is 79.8 Pa and 94.4 Pa, respectively. In Figure 6d, when the shear rate is higher than 47.3 rad s^{-1}, there are several discrete points in the *G''* of 0.5 wt% bagasse-derived NFC aqueous suspension, indicating that the network structure of NFC in the suspension is not stable. For the 0.5 wt% wood-, wheat straw- and bamboo-derived NFC suspension, the tan δ is < 1 throughout the angular frequency scanning range, indicating that the suspensions exhibit viscous behavior. For the 0.5 wt% bagasse-derived NFC aqueous suspension, the tan δ is > 1 when the shear rate is higher than 44.7 rad s^{-1}, further confirming that the entanglement network structure of NFC in the water dispersions is unstable.

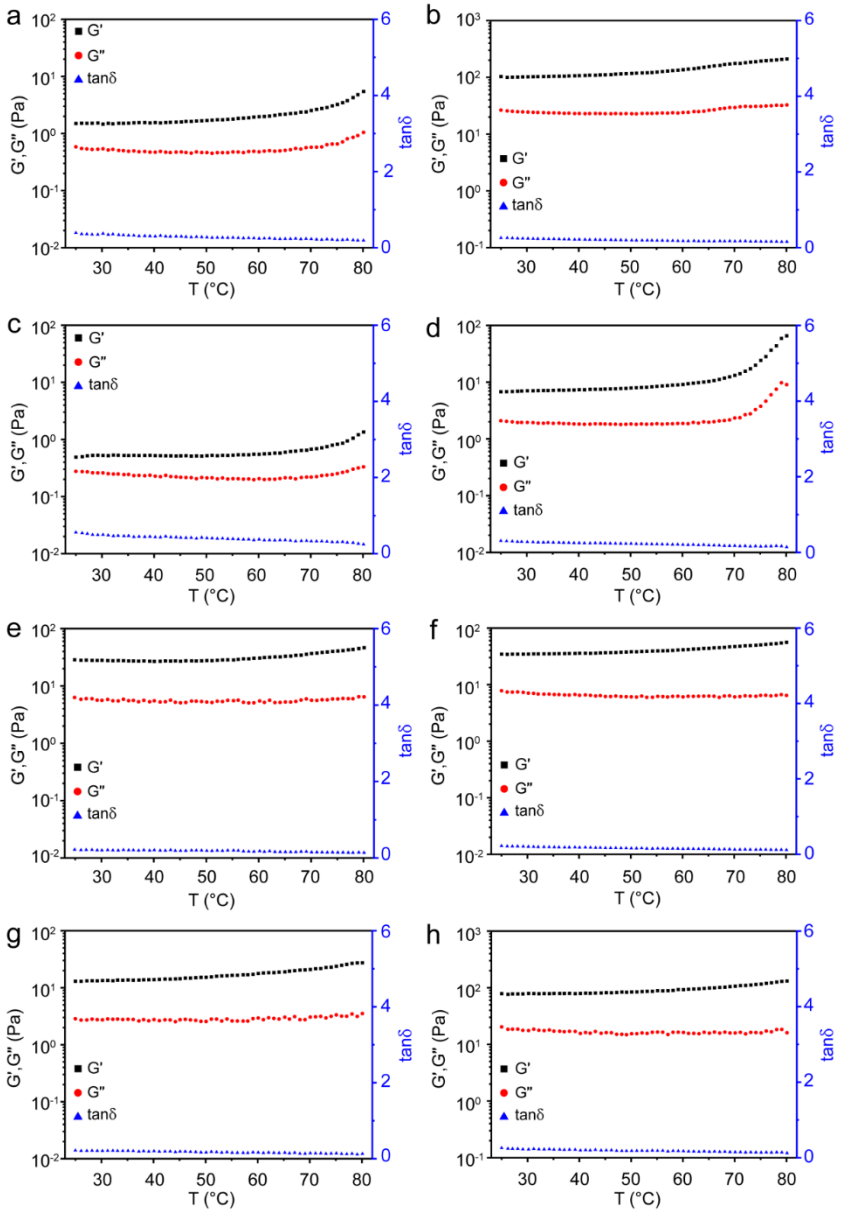

Figure 7. Rheological properties of 0.2 wt% (a, c, e, g) and 0.5 wt% (b, d, f, h) NFC suspensions with increasing the temperature. (a, b) wood, (c, d) bagasse, (e, f) wheat straw, and (g, h)

bamboo.

The rheological properties of NFC suspensions with different concentrations as a function of temperature are shown in Figure 7. For NFC aqueous suspensions with a solid concentration of 0.2 wt%, the storage modulus of all samples is greater than the loss modulus, with tan δ of less than 0.5, even if the temperature increases from room temperature to 80 °C, indicating that the suspension maintains a viscous behavior during the heating process. As temperature increases and some water may evaporate, the *G'* and *G''* of all samples increase slightly. At 80 °C, the *G'* of wood-, bagasse-, wheat straw- and bamboo-derived NFC suspensions reaches 5.5 Pa, 1.4 Pa, 46.5 Pa, and 27.5 Pa, respectively. When the solid concentration of the NFC aqueous suspension is increased to 0.5 wt%, the *G'* and *G''* of the samples increase. During the temperature-rising process, the *G'* of all samples is greater than the loss modulus. The *G'* and *G''* of wood-, wheat straw-, and bamboo- derived NFC aqueous suspensions are relatively stable. The *G'* slightly increases with increasing the temperature. However, for 0.5 wt% bagasse-derived NFC suspension, the *G'* and *G''* of the sample rapidly increase when the temperature is higher than 71 °C. At 80 °C, the *G'* and *G''* of the 0.5 wt% bagasse-derived NFC suspension are 65.5 Pa and 9.1 Pa, respectively. The above results indicate that the rheological properties of NFC aqueous suspension are relatively stable during the rise of temperature. With the increase of temperature, some water in the suspension may evaporate. The *G'* of the suspension thus increases. However, the characters of NFC building blocks have an impact on the rheological properties of the aqueous suspensions.

4 Conclusions

In this study, we individualized high-crystalline NFC from wood, bagasse, wheat straw, and bamboo by chemical pretreatment combined with nanofibrillation using a high-pressure homogenizer. All the NFC suspensions contained web-like entangled 3~5 nm nanofibers and nanofiber bundles. The rheological properties of different biomass resources-derived NFC aqueous suspensions were compared. Although the structures of individual nanofibers in the four types of NFC were very similar, there were still differences in the rheological behavior of their corresponding aqueous suspensions. The storage moduli of all samples were greater than their corresponding loss moduli. When the concentration of the water suspensions increased from 0.2 wt% to 0.5 wt%, both the storage modulus and the loss modulus increased. With the increase of shear rate, the rheological behavior of bagasse NFC suspension had a different trend from other NFC suspensions, indicating that its nanofiber network structure was somewhat destroyed at high shear rate. Temperature had little effect on the rheological properties of NFC aqueous suspensions. However, when the temperature rose to nearly 80 °C, the storage modulus and loss modulus of some suspensions increased.

Acknowledgement: The authors would like to thank Northeast Forestry University for their support.

Funding Statement: This work was supported in part by the Fundamental Research Funds for the Central Universities (2572019BB03 and 2572021CG01), the Startup Fund and the Catalyst Fund from Rowan University and the Research Grant (PC 20-22) from the New Jersey Health Foundation from USA, and the Grant (DMR-2116353) from the National Science Foundation.

References

1. Ling, S. J., Chen, W. S., Fan, Y. M., Zheng, K., Jin, K., Yu, H. P., Buehler, M. J., Kaplan, D. L. (2018). Biopolymer nanofibrils: structure, modeling, preparation, and applications. *Progress in Polymer Science. 85,* 1-56.

2. Chen, W. S., Yu, H. P., Lee, S. Y., Wei, T., Li, J.,Fan, Z. J. (2018). Nanocellulose: a promising nanomaterial for advanced electrochemical energy storage. *Chemical Society Reviews. 47(8),* 2837-2872.

3. Kim, J. H., Lee, D. G., Lee, Y. H., Chen, W. S., Lee, S. Y. (2019). Nanocellulose for energy storage systems: beyond the limits of synthetic materials. *Advanced Materials. 31(20),* 10.1002/adma. 201804826.

4. Dai, M., Zhao, F., Fan, J. J., Li, Q., Yang, Y., Fan, Z. J., Ling, S. J., Yu, H. P., Liu, S. X., Li, J., Chen, W. S.,Yu, G. H. (2022). A nanostructured moisture-absorbing gel for fast and large-scale passive dehumidification. *Advanced Materials. 34(17),* 10.1002/adma. 202200865.

5. Shi, M. J., Bai, L. L., Wan, D. H., Chang, J., Li, Q., Yu, H. P., Liu, S. X., Wei, T., Chen, W. S.,Fan, Z. J. (2022). Transparent and flexible structurally colored biological nanofiber films for visual gas detection. *Matter. 5(9),* 2813-2828.

6. Li, Q., Wang, F., Zhang, Y., Shi, M., Zhang, Y., Yu, H., Liu, S., Li, J., Tan, S. C.,Chen, W. (2023). Biopolymers for hygroscopic material development. *Advanced Materials.* 10.1002/adma. 202209479.

7. Chen, W. S., Yu, H. P., Liu, Y. X., Chen, P., Zhang, M. X.,Hai, Y. F. (2011). Individualization of cellulose nanofibers from wood using high-intensity ultrasonication combined with chemical pretreatments. *Carbohydrate Polymers. 83(4),* 1804-1811.

8. Chen, W. S., Li, Q., Cao, J., Liu, Y. X., Li, J., Zhang, J. S., Luo, S. Y.,Yu, H. P. (2015). Revealing the structures of cellulose nanofiber bundles obtained by mechanical nanofibrillation via TEM observation. *Carbohydrate Polymers. 117,* 950-956.

9. Iwamoto, S., Nakagaito, A. N., Yano, H., Nogi, M. (2005). Optically transparent composites reinforced with plant fiber-based nanofibers. *Applied Physics A-Materials Science & Processing. 81(6),* CP8-1112.

10. Chen, W., Yu, H., Liu, Y., Hai, Y., Zhang, M., Chen, P. (2011). Isolation and characterization of cellulose nanofibers from four plant cellulose fibers using a chemical-ultrasonic process. *Cellulose. 18,* 433-442

11. Chen, W. S., Yu, H. P.,Liu, Y. X. (2011). Preparation of millimeter-long cellulose I nanofibers with diameters of 30-80 nm from bamboo fibers. *Carbohydrate Polymers. 86(2),* 453-461.

12. Chen, W. S., Yu, H. P., Li, Q., Liu, Y. X.,Li, J. (2011). Ultralight and highly flexible aerogels with long cellulose I nanofibers. *Soft Matter. 7(21),* 10360-10368.

13. Chen, W. S., Li, Q., Wang, Y. C., Yi, X., Zeng, J., Yu, H. P., Liu, Y. X., Li, J. (2014). Comparative study of aerogels obtained from differently prepared nanocellulose fibers. *Chemsuschem. 7(1),* 154-161.

14. Uetani, K., Yano, H. (2013). Self-organizing capacity of nanocelluloses via droplet evaporation. *Soft Matter. 9(12),* 3396-3401.

15. Abe, K. (2016). Nanofibrillation of dried pulp in NaOH solutions using bead milling. *Cellulose. 23(2),* 1257-1261.

16. Ho, T. T. T., Abe, K., Zimmermann, T., Yano, H. (2015). Nanofibrillation of pulp fibers by twin-screw extrusion. *Cellulose. 22(1),* 421-433.

17. Isogai, A., Saito, T., Fukuzumi, H. (2011). TEMPO-oxidized cellulose nanofibers. *Nanoscale. 3(1),* 71-85.

18. Sydney Gladman, A., Matsumoto, E. A., Nuzzo, R. G., Mahadevan, L.,Lewis, J. A. (2016). Biomimetic 4D printing. *Nature Materials. 15(4),* 413-418.

19. Chen, Y., Yu, Z. Y., Ye, Y. H., Zhang, Y. F., Li, G. Y.,Jiang, F. (2021). Superelastic, hygroscopic, and Ionic conducting cellulose nanofibril monoliths by 3D printing. *ACS Nano. 15(1),* 1869-1879.

20. Moberg, T., Sahlin, K., Yao, K., Geng, S., Westman, G., Zhou, Q., Oksman, K., Rigdahl, M. (2017). Rheological properties of nanocellulose suspensions: effects of fibril/particle dimensions and surface characteristics. *Cellulose. 24,* 2499-2510.

21. Qu, R. J., Wang, Y., Li, D., Wang, L. J. (2021). The study of rheological properties and microstructure of carboxylated nanocellulose as influenced by level of carboxylation. *Food Hydrocolloids. 121,* 10.1016/j. foodhyd. 2021.106985.

22. Atakhanov, A. A., Kholmuminov, A. A., Mamadierov, B. N., Turdikulov, I. K., Ashurov, N. S. (2020). Rheological Behavior of Nanocellulose Aqueous Suspensions. *Polymer Science Series A. 62(3),* 213-217.

23. Dimic-Misic, K., Vanhatalo, K., Dahl, O., Gane, P. (2018). Rheological proerties comparison of aqueous dispersed nanocellulose derived from a novel pathway-produced microcrystalline cellulose or by conventional methods. *Applied Rheology. 28(6),* 10.3933/ApplRheol-28-64474.

24. Chirayil, C. J., Mathew, L., Hassan, P. A., Mozetic, M., Thomas, S. (2014). Rheological behaviour of nanocellulose reinforced unsaturated polyester nanocomposites. *International Journal of Biological Macromolecules. 69,* 274-281.

25. Segal, L., Creely, J. J., Martin Jr, A. E., Conrad, C. M. (1959). An empirical method for estimating the degree of crystallinity of native cellulose using the X-ray diffractometer. *Textile Research Journal. 29(10),* 786-794.